Chapter 18
Comparison of SIMS and MALDI for Mass Spectrometric Imaging

John S. Hammond

Abstract Secondary ion mass spectrometry (SIMS) has become a highly refined and widely used mass spectrometric technique for the two- and three-dimensional (3D) imaging of inorganic materials, especially for the semiconductor industry. The optimization of primary ion sources for ultrahigh spatial resolution, very high transmission and high mass resolution analyzers, and specialized sample handling, particularly for wafers, has resulted in the widespread utilization of SIMS instruments for materials research and quality control in the semiconductor and magnetic materials industries. The utilization of SIMS for mass spectrometric imaging of organic and biological samples has trailed the applications for inorganic materials because of the need to improve the sub-micrometer molecular spatial resolution capabilities of SIMS that are now commonplace for inorganic and semiconductor SIMS analysis. The rapid improvements in matrix-assisted laser desorption/ionization (MALDI) for imaging macromolecular species, particularly for tissue cross sections, are now being limited by the fundamental spatial resolution capabilities of the laser desorption process. A comparison of the new developments of SIMS and MALDI instrumentation points out that these two techniques are complementary in many capabilities, especially ultimate spatial resolution and molecular mass range. An overview is presented of the SIMS process, primary ion sources, mass analyzers, and software for mass spectrometric imaging of organic and especially biological samples. Examples of the analysis of tissue cross sections, imaging resolution of subcellular features, and 3D imaging of drug delivery materials illustrate the potential for SIMS and MALDI to become invaluable complementary techniques for future mass spectrometric imaging.

J.S. Hammond (✉)
Physical Electronics, 18725 Lake Drive East, Chanhasse, MN 55317, USA
e-mail: JHammond@phi.com

M. Setou (ed.), *Imaging Mass Spectrometry*: *Protocols for Mass Microscopy*,
DOI 10.1007/978-4-431-09425-8_18, © Springer 2010

18.1 Introduction

Secondary ion mass spectrometry (SIMS) has become a highly refined and widely used MS technique for the two-dimensional (2D) and three-dimensional (3D) imaging of inorganic materials, especially in the semiconductor industry. The optimization of primary ion sources for ultrahigh spatial resolution, very high transmission and high mass resolution analyzers, and specialized sample handling – particularly for wafers – has resulted in the widespread utilization of SIMS instruments for materials research and quality control in the semiconductor and magnetic materials industries. The use of SIMS for the MS imaging of organic and biological samples has trailed applications for inorganic materials because of the need to improve the submicrometer molecular spatial resolution capabilities of SIMS – capabilities that are now commonplace in inorganic and semiconductor SIMS analysis. Rapid improvements in matrix-assisted laser desorption/ionization (MALDI) for imaging macromolecular species, particularly for tissue cross sections, are now being limited by the fundamental spatial resolution capabilities of the laser desorption process. A comparison of new developments in SIMS and MALDI instrumentation indicates that these two techniques are complementary in many ways, especially with respect to the ultimate spatial resolution and molecular mass range. An overview is provided here of the SIMS process, primary ion sources, mass analyzers, and the software used for the MS imaging of organic and especially biological samples. Examples of the analysis of tissue cross sections, the imaging resolution of subcellular features, and the 3D imaging of drug delivery materials illustrate the potential for SIMS and MALDI to become invaluable complementary techniques in undertaking future MS imaging procedures.

18.2 SIMS Overview

18.2.1 Analytical Overview

In SIMS, a primary ion beam is directed to the sample surface to induce a collision cascade in the near-surface region. A portion of the energy from this collision cascade is redirected toward the surface, thus promoting the release of atoms, molecules, and molecular fragments into the vacuum system of the SIMS instrument. This release of surface material is commonly referred to as the sputtering process. A fraction of the sputtered material emerges from the sample as positively or negatively charged species; these are then extracted into a mass spectrometer, where ions are separated on the basis of their respective mass-to-charge ratios.

The ejected ions are collected by a high-performance mass spectrometer. Today, two types of spectrometers are used in MS imaging: a time-of-flight (TOF) analyzer and a magnetic sector analyzer. Each of the current analyzer designs collects about 50% of the emitted ions and can provide a mass analysis with an ultrahigh

mass resolution [i.e., >15,000 M/Δm full-width at half-maximum (FWHM)]. The magnetic sector analyzer separates and counts, in a parallel fashion, a limited number of different mass-to-charge species, depending on the number of detectors in the detection system. The TOF analyzer, coupled with a pulsed primary ion gun, separates all the ions as a function of their flight time; it can therefore collect the full mass range of emitted secondary ions.

The imaging capabilities of current commercial SIMS instruments is based on the use of scanning microprobe primary ion sources, with beam diameters as small as 50 nm. The use of scanning primary ion beams that are completely computer controlled and synchronized with a TOF or magnetic sector mass spectrometer allows for the collection of mass spectra or ion-selected images over the field of view defined by the user. The advantage of the TOF-SIMS design is the parallel collection of ion images from all the different ion species, although the ultimate spatial resolution and analytical speed for a single mass-selected ion image does not equal the ultimate spatial resolution performance of the magnetic sector-designed SIMS instruments. Commercially available SIMS instruments include software programs that provide enhanced image presentations and a range of image analysis capabilities.

It is beyond the scope of this text to provide a comprehensive discussion of all aspects of the historical development, instrumentation engineering details, and sophisticated data interpretation available for SIMS analysis. For more detail, the reader is referred to two of several available treatises on this subject [1, 2].

18.2.2 Primary Ion Sources and Ion Creation

Figure 18.1 shows a schematic representation, produced by molecular dynamics simulation calculations, of the impact of a 15-keV Ga primary ion into an Ag-111 crystal, as well as the resultant energy cascade [3].

This simulation illustrates several key points concerning the SIMS process. First, the primary ion releases energy below the surface of the sample in the energy cascade. This released energy can result in significant damage to chemical bonds and the molecular structure. A portion of the energy cascade reaches the sample surface and initiates the sputtering process. For this reason, initial SIMS experiments that aimed to obtain molecular spectroscopy and molecular imaging without chemical or molecular damage limited the primary ion dose to 1% of the surface atoms, or 10^{13} ions/cm^2. This was defined as the static limit for static SIMS (SSIMS), and it was intended to ensure that no primary ion struck a point on the sample surface that had already sustained a previous ion impact. Second, the number of sputtered atoms, which is dependent on the primary ion mass and kinetic energy and the composition of the sample, is relatively low. In the foregoing simulation, only 29 atoms were sputtered for each incoming primary ion. In addition, the probability of atoms or molecular fragments leaving the sample surface as ions is also dependent on the chemical composition of the sample. For some inorganic compounds,

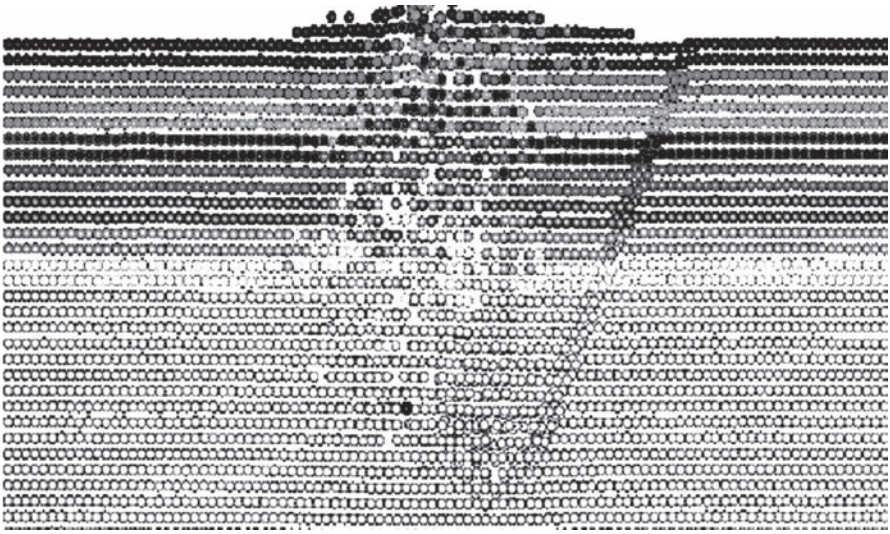

Fig. 18.1 Molecular dynamics simulation of impact of a 15-kV Ga ion into Ag, after 29 ps

the probability of ion formation during sputtering can approach unity; for many molecular species, especially large organic species, the probability can be as low as 10^{-3}. The variability of the probability of ion formation with changes in surface composition has led to the working premise that SIMS is a nonquantitative technique and that changes in intensity among SIMS images could result from both the change in ion formation probability and the surface coverage. Its low ion formation probability has led many researchers to suggest that imaging SSIMS for organic and biological samples may be limited to a spatial resolution of 1 μm.

The separation of the primary ion point of impact and the point of secondary ion emission is suggested in the molecular dynamics simulations of Fig. 18.1 and further illustrated in Fig. 18.2.

This illustration has been explored in greater analytical detail by several research groups, including a recent publication by Delcorte and Garrison [4].

The coincidence within 10 nm of the primary ion impact and large mass molecular ion fragment emission points to the potential for SIMS to provide excellent spatial resolution for MS imaging. For this reason, early SIMS instruments sought to use highly focused scanning primary ion sources. Although a highly focused Cs ion beam source with a minimum beam diameter <50 nm is used with the Cameca nanoSIMS 50 instrument [5], most SIMS instruments use a liquid metal ion gun (LMIG) as the source for primary ions. The Cs source in the Cameca nanoSIMS 50 operates with a rastered DC beam, which can provide outstanding spatial resolution for atomic secondary ions but is generally not useful for organic or molecular species; for this reason, the nanoSIMS 50 is not discussed further in this chapter.

The early LMIG sources for SIMS instruments all used a Ga ion emitter. When used in conjunction with a TOF analyzer, the LMIG must be pulsed at each pixel

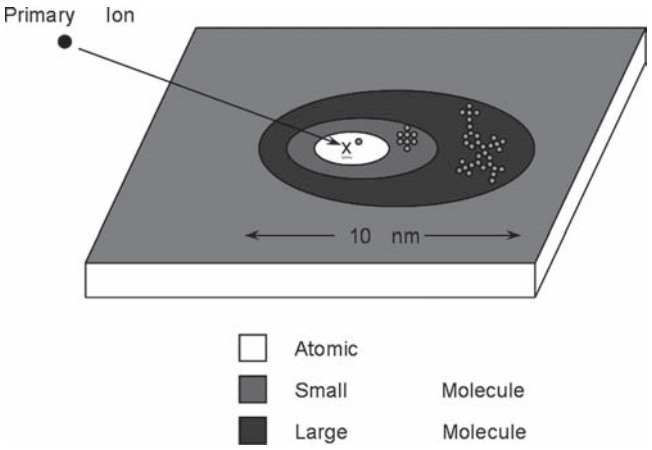

Fig. 18.2 Sites for atomic, small, and large molecular ion ejections, relative to primary impact site

of the scanned image over the sample surface. The time-duration of this pulse is generally <1 ns for high mass resolution spectroscopic data. In the imaging mode, the Ga-emitting LMIG sources can routinely produce a pulsed beam diameter <100 nm, with slightly degraded mass resolution performance. This performance is highly useful for most inorganic and semiconductor samples. However, because of the low sputter yield and ionization efficiency of Ga primary ion sources, the practical limit for MS imaging on organic and biological samples has been ~1 μm.

To improve both the higher mass fragment sputter yield efficiency by the primary ion and the probability of ionization in the sputtered species, both of which are important for improving the ion-counting statistics necessary for the imaging spatial resolution of organic and biological samples, alternative primary ion sources are being explored. A summary of the presently available micro-focused pulsed primary ion sources for SIMS imaging is shown in Table 18.1. The relative ion yield efficiency is based on the relative number of high mass secondary ions (mass of *m/z* 300–400) of species from thick samples of organic films. The same number of primary ions was used for all measurements. The relative ion yields and the efficiency of secondary ion formation are important for the optimization of imaging SIMS experiments. It should be noted that the absolute numbers shown in Table 18-1 can change by about 50%, depending on the sample used. The key trends are that the relative ion yield is a nonlinear function of the mass of an atomic ion, and the use of a higher number of atoms in a cluster ion source also produces a dramatic nonlinear increase. To date, a C_{60}^+ source has been found to produce the highest relative ion yield for species from most thick organic materials, but the spatial resolution in a scanning pulsed microprobe mode is still limited to about 1 μm. The relative ion yield of the C_{60}^+ primary ion source is sufficiently high that the ion imaging spatial resolution may approach 100 nm, if improved primary ion source optics or new imaging analyzers can be developed.

Table 18.1 Performance of pulsed imaging ion sources [6]

Primary ion species	Ion mass a.m.u.	Relative ion yield efficiency	Best pulsed spatial resolution (μm)
Ga^+	69	1	80
In^+	115	3.5	100
Au^+	197	22	100
Bi^+	208	n.a.	100
Au_2^+	394	190	130
Bi_2^+	416	n.a.	n.a.
Au_3^+	591	270	130
Bi_3^+	624	n.a.	100
C_{60}^+	720	520	1,200

n.a. not applicable

18.2.3 SIMS Analyzers

Presently, two commercial designs are used for the TOF-SIMS MS imaging of organic and biological samples. The first is a reflectron design, which is second-generation TOF optics that was introduced after the initial introduction of TOF-SIMS instruments which used the Poschenrieder mass analyzer design [2]. The reflectron design has been refined in several models and is presently commercially available as the TOF.SIMS 5 from ION-TOF GmbH [7]. A schematic of this instrument is shown in Fig. 18.3.

The third-generation TOF-SIMS instrument is based on a triple focusing time-of-flight (TRIFT) mass analyzer [8]. This instrument is commercially available from Physical Electronics USA and ULVAC-PHI. A schematic diagram of this instrument is shown in Fig. 18.4.

Both analyzers provide similar high mass resolution and high collection efficiency for a broad mass range of secondary ions. In each instrument, the secondary ions are generated by a short time-duration pulse of highly focused primary ions. When they leave the sample surface, the ions have a spread of kinetic energy and angular distribution as a result of the primary ion energy cascade. To enhance the collection efficiency of the analyzer, the ions are focused through a high-voltage extraction field into the first lens of the analyzer. Due to the short time pulse of the primary ion beam, all mass ions leaving the sample are assumed to depart at $T=0$. All secondary ions are accelerated through the same voltage, such that the extraction voltage equals 0.5 mv^2. The mass-to-charge ratio of each secondary ion will then be proportional to the square of the flight time to the detector. By using a series of low-mass/charge ions that appear in all spectra, the recorded flight times for all ions can be converted to exact masses. In both analyzers, the range of kinetic energy levels of the emitted secondary ions is minimized by the energy compensation trajectories inside the analyzer. The reflectron uses an ion mirror that allows ions with slightly higher kinetic energy levels to have longer flight paths into the ion mirror before their flight trajectories are "reversed" back to the detector. In the TRIFT

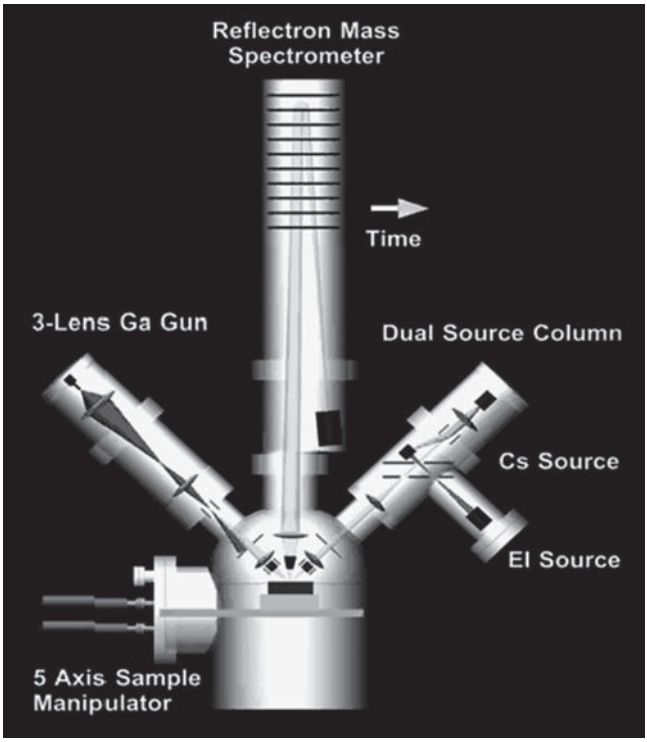

Fig. 18.3 Schematic of the TOF.SIMS 5

analyzer, secondary ions with higher kinetic energy levels traverse slightly larger radius trajectories, through the three 90° electrostatic sectors, before reaching the detector. By using either of these energy compensation techniques, the ions with the same *m/z* that start to diverge at the start of the flight path end up converging at exactly the same flight time at the detector; this allows for a very high mass resolution. By using a detector with a typical 20-kV value post acceleration, either of these two analyzers can achieve a mass resolution >15,000 M/Δm FWHM, with a mass range over *m/z* 10,000.

18.2.4 Two-Dimensional Analyses

As previously described in Sects. 18.2.1 and 18.2.2 (above), the pulsed microprobe ion beam can be scanned at the surface of the sample and the secondary ions of all masses are collected in a parallel manner by the TOF analyzer. The computer data system therefore records a matrix of the detected ions, with each detected ion labeled in the *x*- and *y*-positions of the primary ion beam and the flight time, *t*, of the ion to the detector. The calibration of the analyzer allows the time, *t*, to be

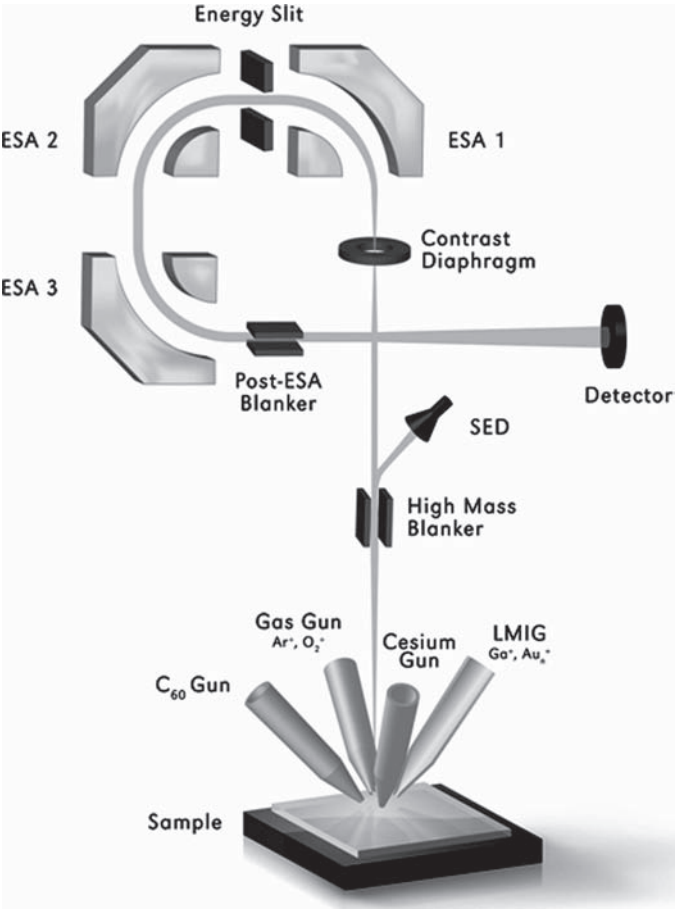

Fig. 18.4 Schematic of the PHI TRIFT V *nanoTOF* TOF-SIMS

converted into the mass of the detected ion. This matrix of data is referred to as the "raw file," and it is used for retrospective 2D image analyses. Depending on the optical constraints of the primary ion gun, the size and number of the *x* and *y* pixels in the image, and the desired mass range – and therefore the pulsed repetition rate of the analyzer – a SSIMS 2D raw file usually requires 15–30 min to acquire data for a typical 100 μm × 100 μm surface image.

The flow process of the retrospective data analysis of the raw file is illustrated in Fig. 18.5. The user can select four different modes of data interpretation, each of which is briefly described next. These four forms of output are (1) total ion image, (2) total area spectrum, (3) regions of interest spectra, and (4) mass-specific images.

For MS imaging, probably the most important analytical question is how many different regions exist on the sample of interest. This can be answered, to a first approximation, by displaying the total ion image. For the total ion image, the software

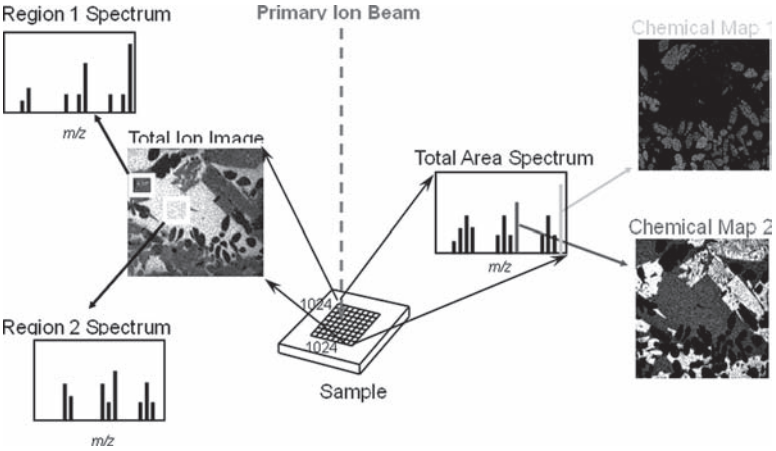

Fig. 18.5 Flow process for two-dimensional (2D) image analysis, using retrospective data analysis of a raw file

sums the number of ions, regardless of mass-to-charge ratio, at each pixel in the image. Normally, the different total ion intensity levels are displayed using a pseudo-color histogram routine; the areas of the image with the same color may then be assumed to be areas with similar chemical or molecular compositions. The total ion image can then also act as a "roadmap" for the locations or "regions" that may be targets for additional MS interrogation.

The second question is how many different chemical and molecular species exist within the imaged area. The software will sum all the ions of the same mass, regardless of *x*- and *y*-positions, from the raw file, thus producing a total area spectrum. The peaks in this spectrum can then be assigned by using exact mass assignments, by using comparisons with mass fragment libraries and standard molecular spectra that are available within the commercial TOF-SIMS software, or by using search engines in the system software to compare the total mass spectrum with reference spectra available from third-party sources (e.g., SurfaceSpectra [9]).

The third question is to identify the chemical and molecular compositions within specific regions of interest, identified using the total ion image. The location of the desired pixels located within a region can be selected manually by the user, using the total ion image as a roadmap, or the software can use the intensity values of the pixels for the histogram threshold selection of pixel locations. By summing the spectra from multiple pixels with the same range of total ion intensity over the original total ion image, excellent spectra can usually be reported from each region of interest. These spectra can then provide classifications for all regions of interest.

The final question is about obtaining images for each of the selected chemical or molecular species. One single peak – or a "fingerprint" of multiple peaks associated with one particular species – can be used to create a mass-selected image. The number of mass-selected images can then equal the number of species on the surface of the sample.

18.2.5 Depth Profile Analysis and 3D Analyses

As noted in the earlier section on ion creation (Sect. 18.2.2), the TOF-SIMS technique measures ions that usually originate from the outermost one to two atomic or molecular layers. Although the energy cascade process can disturb the chemical and molecular bonds below the surface in most organic and biological samples, many samples of metal, semiconductor, ceramic, and other inorganic materials can retain their elemental and chemical compositions, despite the affects of the energy cascade introduced by the primary ion beam. In the TOF-SIMS experiment, the short time-duration of the pulsed ion beam sputter removes a fraction of a monolayer during the typical MS analysis. However, for many inorganic samples, the experimenter is interested in gradients of composition, from the outermost surface to microns in depth. In addition, by combining the 2D imaging discussed in the previous section with an effective method of profiling the sample as a function of depth, a method of rendering 3D characterizations can be obtained. To facilitate a reasonable experimental time-duration and maintain high spatial resolution, high mass resolution, and high sensitivity in the TOF-SIMS analysis, the dual-beam approach to depth profiling is normally utilized. In this approach, one ion beam is used to produce secondary ions for SIMS analysis, and a second ion beam is provided for rapid sputter removal of the sample surface. This approach is illustrated in Fig. 18.6.

In the dual-beam approach, the MS analysis of the surface is based on the pulsed primary ion beam. Typically, the pulsed primary ion beam is rastered over a region of the sample, to acquire a raw file of the first layer. The computer control of the system then suspends the TOF-SIMS data acquisition and initiates a second DC

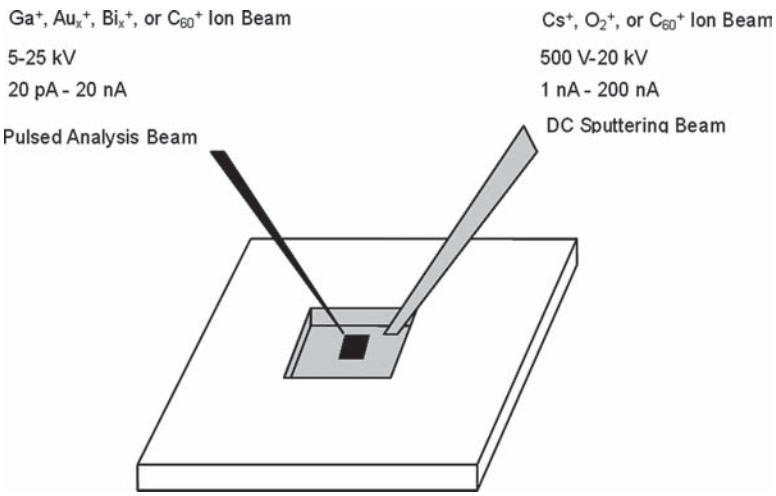

Fig. 18.6 Schematic of the dual ion beam approach to TOF-SIMS depth profiling and 3D analyses

beam to be rastered over a slightly larger area of the sample, to remove by sputtering a user-defined thin layer of the sample. After this layer is removed, the second ion beam is suspended and the pulsed primary ion beam is again used to acquire a second image raw file of freshly exposed surface. This process is alternately continued until a sputter depth profile to the desired depth has been obtained.

One significant advantage of the dual ion beam approach is that the composition and kinetic energy of the DC sputter beam can be selected to achieve a high sputter rate, with a minimum penetration depth of the energy cascade. In general, the lower the impact voltage of the DC sputtering ion beam, the lower will be the penetration depth of the energy cascade; this minimizes artifact formation within the composition of the sputter-exposed surface layers. In addition, the probe size and ion current of the sputter ion beam are both kept relatively large to promote rapid depth profiling; meanwhile, the probe size and ion current of the primary ion beam are kept small, to obtain optimal spatial resolution and optimal MS performance.

The depth profiling of organic and biological materials, in contrast to the depth profiling of inorganic materials, has not been successful when using monatomic ions. This failure has generally been attributed to the destruction of the chemical and molecular structure within the sample by the penetration of the energy cascade below the surface of the sample, as noted in Fig. 18.1. In the pioneering work of Gillen et al. in 1998 at NIST, the concept of organic and molecular depth profiling using cluster ion sources was demonstrated using polyatomic SF_5^+ and C_n^- primary ion sources [10]. Although sputter yields, secondary ion yields, and the potential for organic and molecular depth profiling have been studied for a large number of different polyatomic and cluster ion sources [11], C_{60}^+ is the most commonly used primary cluster ion source in use today, which is the result of its relatively high secondary ion yield and its commercial availability as a robust source; it also has favorable scanning microprobe and pulsed source capabilities [12].

The molecular dynamics simulations by Garrison et al. of the impact of a C_{60}^+ primary ion on a model Ag substrate, as shown in Fig. 18.7, illustrates key points vis-à-vis the success of molecular depth profiling [3]. The first point is the very large number of sputtered Ag atoms from the impact of one C_{60}^+ ion. In comparison with 21 atoms sputtered with the 15-keV Ga^+ primary ion, the 15-keV C_{60}^+ primary ion sputters 324 atoms. This sputter rate enhancement is even more pronounced when using one of many polymer systems, where the sputter rate of most polymers is eight times the sputter rate of SiO_2 under the same C_{60}^+ sputtering conditions [13]. This extremely high sputter rate is thought to originate from the overlapping of the energy release from each of the 60 carbon atoms that result from the impact-induced fragmentation of the C_{60}^+ cluster ion. The second point is that the depth of energy deposition is approximately the depth of the sputter crater; this means that breaks in chemical bonds and modifications to the molecular structure of the sample occur in a region where the sample material will be sputtered away. The resultant surface after C_{60}^+ sputtering will present a composition that resembles the original composition, making it ideal for molecular depth profiling. The third point is that the C_{60}^+ primary ion fragments are not implanted deeply in the sample – as noted for the Ga^+ ion, which remains in the sample after the sputtering process (see Fig. 18.1).

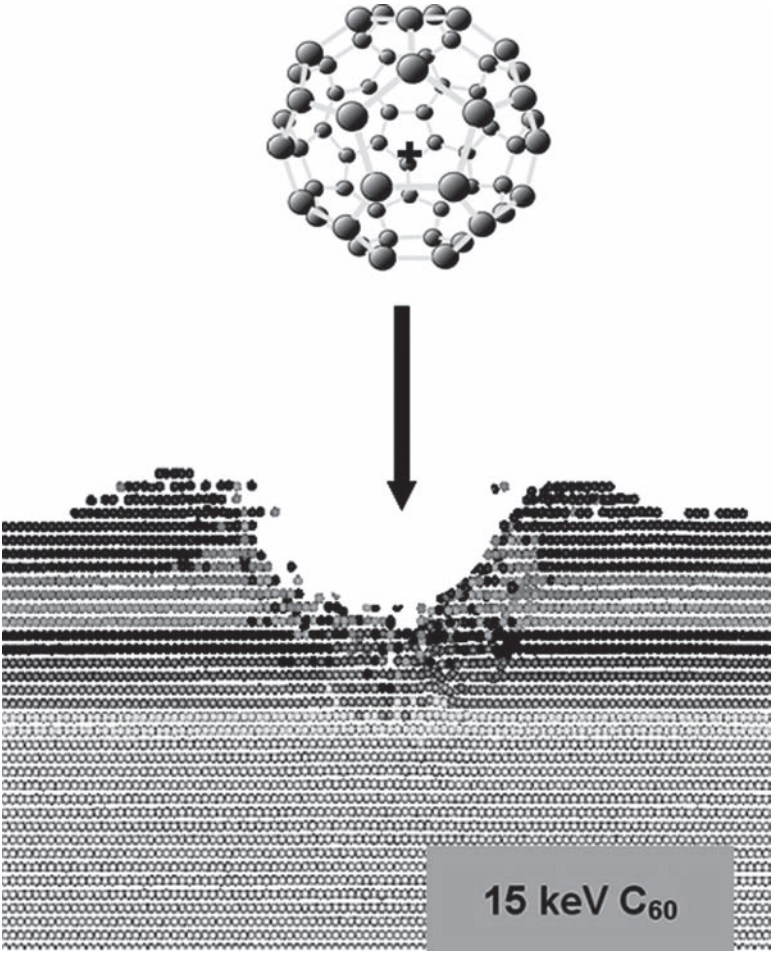

Fig. 18.7 Molecular dynamics simulation of impact of 15-kV C_{60}^+ ion into Ag after 29 ps

In fact, most of the C atoms from the C_{60}^+ primary ion are removed in the sputter process. However, recent C_{60}^+ depth profiles on model polymers now suggest that the eventual accumulation of carbon at the bottom of the sputter crater may be responsible for terminating successful TOF-SIMS molecular depth profiling [14]. The depth of this termination depends on the organic material used and the energy of the incident C_{60}^+ primary ions. However, molecular depth profiles from 1 to 3 μm can be practical for many samples. The fourth point is that the depth profile induces a slight roughening to the organic material consequent to the very high sputter rate for each impacting ion: this has been observed by comparisons of atomic force microscopy (AFM) measurements of the outer surface and the crater bottom of the C_{60}^+ depth profile of thick polymer films [14].

The data acquisition of 3D images uses a combination of analytical protocols used for 2D retrospective TOF-SIMS imaging discussed earlier and the interleaved TOF-SIMS depth profiling that is highly successful with inorganic multilayer samples. The microprobe primary ion gun is rastered over the sample and data for all secondary ions, produced at each pixel, are recorded in the matrix of a raw file, together with the coordinates of the *x* and *y* for pixel position, *t* for the flight time to the detector, and *c* for the sputter cycle. After recording the first 2D image, the user-defined length of rastered sputtering of the organic material by the C_{60} ion gun will remove the desired thickness of the sample. The process is then repeated for the next sputter cycle to produce a series of image slices as a function of depth into the material. The user then retrospectively displays the data, using the same software routines used in the 2D analysis, except that the axis of depth is added to the display.

For the visualization of 3D structures, the software function of iso-surface structure modeling can be highly useful. In this routine, the user selects a maximum and minimum intensity for a particular mass or fingerprint of masses. These intensity thresholds are then used to determine which pixels will be grouped together from the *x*, *y*, and *c* coordinates matrix of the 3D raw data file, to construct a 3D model. The iso-surface models can then be displayed using color-coding and a color opacity level. The user can then overlay as many models as desired in a 3D rendering of the sample. The overlaid models can be displayed on the computer screen, using 3D axis rotation to identify the 3D locations of the coincidence or anticoincidence of different molecular species. An example of this 3D analysis is presented later in this chapter, with reference to the analysis of drugs in a drug-eluting polymer coating used on a medical stent.

18.2.6 Sample Preparation

Because of the excellent surface sensitivity of the TOF-SIMS technique – i.e., generally one to two atomic layers or one molecular layer – the cleanliness of the sample preparation is of extreme importance. It is beyond the scope of this chapter to cover all the important details regarding sample cleanliness; instead, the reader is referred to an excellent treatise on this topic by Reich [15].

The preparation of samples for MS imaging of organic and biological samples deserves some additional comments. The first covers the imaging of tissue samples. Most of these samples are thin, cross-sectioned samples prepared with a cryomicrotome. The techniques are similar to the sample preparation techniques used for MALDI cross-section samples, and the reader is referred to earlier chapters in this book (Chaps. 1–8). However, it cannot be stressed enough that the cleanliness of the microtome blade will have a dramatic impact on the level of contamination detected in the TOF-SIMS spectra. The use of a freshly cleaned glass blade is therefore recommended.

Following cross-sectioning, the sample can be introduced into the TOF-SIMS vacuum system. All commercial TOF-SIMS instruments now have optional controlled

temperature sample loading locks for sample evacuation and controlled temperature analysis stages. These sample handling systems allow the samples to be introduced into the ultrahigh vacuum chamber and analyzed without the loss of volatile sample components; it does so by using liquid nitrogen cooling hardware, together with heating, to actively control the sample temperature. The addition of heating and liquid nitrogen cooling allows the sample temperature to be maintained at an optimal temperature. It also prevents the buildup of ice on the sample surface, which can result from the condensation of water vapor from inside the vacuum system onto a cold sample surface.

The second issue is how the effects of different ion yields that complicate the intensity levels observed in TOF-SIMS imaging can be ameliorated. This is confounded by the desire to increase the secondary ion yield to achieve higher sensitivity and better spatial resolution based on better imaging statistics. One technique is based on the addition of typical MALDI organic matrix species, to enhance the SIMS analysis. The initial work of Wu and Odom was based on the mixing of peptides and oligonucleotides with 2,5-dihydroxybenzoic acid (DHB). The results indicated that ion yield enhancements for species up to *m/z* 10,000, ranging from 25- to 1,000-fold, could be observed [16]. The early work of Wu did not, however, address the improved imaging made available by this technique. Other research groups, including Heeren et al., used electrospray to apply extremely fine (<1 μm diameter) crystals of DHB on cryosections of the cerebral ganglia of the freshwater snail *Lymnaea stagnalis*. Good images were obtained using an $^{115}In^{+}$ LMIG primary ion source to obtain molecular maps of cholesterol and the neuropeptide APGWamide, with a spatial resolution to <3 μm and a high mass sensitivity to 2,500 Da [17]. The addition of DHB appears to enhance the ion formation of molecules and molecular fragments sputtered by the primary ion beam. It is noteworthy that the mass range of the detected molecular species is limited to much less than 10,000 Da, probably reflecting the limitation of the sputtering process in desorbing molecules of higher molecular weights.

A similar enhancement process is based on the coating of organic materials and tissue cross sections with ultrafine gold and silver particles. Bertrand et al. explored the use of a 2-nm-thick gold metallization to enhance the ionization probabilities for a series of thick polymers and additives with molecular weights in the 1,000- to 5,000-Da range. The results indicated dramatic increases in ion yield of more than two orders of magnitude and enhancements in the number of both gold cationized molecular ions and noncationized ions, using a 15-keV Ga^{+} LMIG primary ion beam. The enhancement was dependent on the polymer species [18].

Ron Heeren et al. combined the deposition of gold with the application of traditional MALDI matrix crystals to enhance the imaging of tissues and cells. For the analysis of tissue cross sections prepared by cryomicrotomy, the deposition of gold resulted in gold islands on the order of 100 nm, as observed with AFM. For the analysis of single neuroblastoma cells grown on glass slides and then frozen and dried, DHB was applied by electrospray to produce small (0.3–1 μm) matrix crystals on the surface of the cells. The imaging of these cells, called matrix-enhanced (ME)-SIMS, produced enhanced lipid molecular ion images of the single cells.

The SIMS signal intensities for this sample preparation produced excellent intact molecular ion imaging of phosphatidylcholine and sphingomyelin at the cellular level. A second group of cells was coated by electrospray with DHB and then subsequently coated with 1-nm films of gold. The imaging of these cells, called metal-assisted (MetA) SIMS, showed strongly enhanced signal intensities for higher spatial resolution imaging. In addition, additional peaks in the mass range of *m/z* 600–1,300 were observed. The spectral resolving power of the MetA-SIMS was about 1 μm, as a result of the convolution of the spatial resolution of the TOF-SIMS instrument and the metal and matrix-assisted signal intensity needed for imaging. The deposition of the thin layer of gold appeared also to decrease the surface diffusion and improve the spatial resolution, compared to the ME-SIMS sample preparation [19].

18.3 Applications of TOF-SIMS Imaging

18.3.1 Tissue Cross-Section Analyses

The wide-ranging success of TOF-SIMS for imaging inorganic and semiconductor materials has led several research groups to explore the potential of TOF-SIMS in imaging cross sections of tissue samples and, ultimately, to focus on subcellular features in cells. The aim of this chapter is not to review all these efforts but rather to provide a selection of examples that illustrate the success and future potential stemming from these research efforts. The preparation of thin cross-section tissue materials has been developed for scanning electron microscopy, transmission electron microscopy, and fluorescence microscopy techniques, and the reader is referred to one of several texts for details of this sample preparation methodology [20].

One of the early efforts to examine TOF-SIMS images of tissue samples was by Wu et al. at Lawrence Livermore National Laboratory, University of California. The sample used was a microtome cross section of a 16-day-old mouse embryo that had been embedded in paraffin. Total ion TOF-SIMS images and selected ion images of the selected areas of the embryo are shown in Fig. 18.8. The TOF-SIMS total ion images of the different organs within the cross section, as well as the selected ion images of different structures in the embryo, suggested that TOF-SIMS could be a useful MS tool in characterizing tissues.

A primary goal of Wu's early research was to explore if TOF-SIMS could differentiate between organs, based on the mass spectra of different regions. The mass spectra in this research were not acquired with a higher mass primary ion cluster source, which would have resulted in abundant low mass fragment peaks, but a lack of the desired molecular peaks. The resultant spectra therefore showed an overlay of the TOF-SIMS fragmentation patterns from many of the different molecular species in each region, rendering an overall "similar" look across the different spectra. Wu et al. [21] used the approach of principal component analysis (PCA) to look for components in the spectra that could separate the areas based on interpretations of multivariate analysis. In Fig. 18.9, the intensity of the Ca^+ or Na^+ images from bone

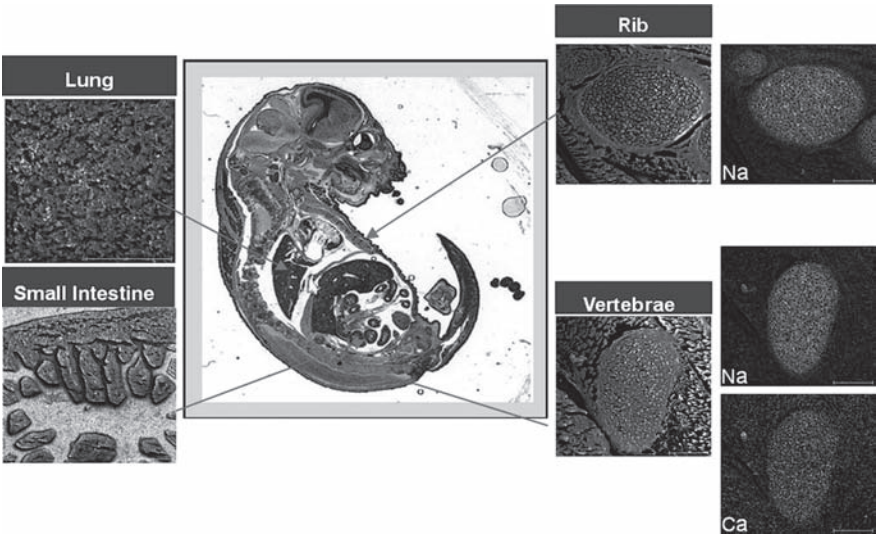

Fig. 18.8 Optical image of the cross section of a 16-day-old mouse embryo embedded in paraffin, with selected area total ion and selected ion TOF-SIMS images

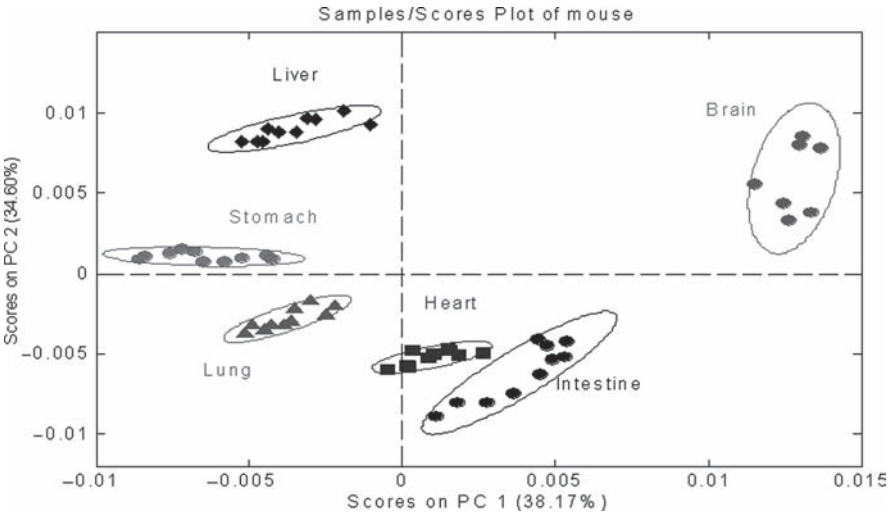

Fig. 18.9 Principal component analysis (PCA) separation of mass spectra from regions of six different organs in a 16-day-old mouse embryo. *PC* principal component

structures can be directly correlated with the optical image. For soft tissues, no single peak can uniquely define an organ structure. In PCA, a fingerprint of different peaks is defined as 1 eigenvector for the matrix of mass and intensity data. By plotting the loading scores for the first PC – i.e., the component that includes

the highest variance in the matrix of data – versus the loading scores for the second PC as a function of the *x* and *y* locations in the image, a multivariate analysis can uniquely separate the regions of the liver, stomach, lung, heart, intestine, and brain in the embryo.

As encouraging as these data are regarding the future of TOF-SIMS imaging of tissue samples, several questions remain. The first question is the identity of the molecular constituents in each area. These data show only the pattern of low mass fragments, not molecular species. The second question is the origin in the cell of these fragment species. The cell membranes are primarily lipid structures; do the TOF-SIMS data show mass fragment differences in the lipid structures or differences in molecules attached to the lipid structures, or do the TOF-SIMS data also sample some of the intracellular material that allows differentiation of the organs [19]?

To further the molecular specificity and spatial resolution of TOF-SIMS imaging of tissue cross-section samples, Laprévote et al. [22] analyzed a 15-μm-thick cross section of a rat brain cut at a temperature of ~–20°C, stored on a stainless steel mount at ~–80°C, and vacuum-dried at room temperature immediately before TOF-SIMS analysis. Based on the expected increase in the secondary ion yield resulting from the use of an Au_3^+ primary cluster ion source, the sample was not coated with a matrix such as DHB or a nanometer film of gold. Fig. 18.10 shows an excellent complementary image of phospholipid ions and cholesterol ions with a 30-min stage rastered image over an 8 mm × 8 mm area, with a pixel resolution of 62.5 μm × 62.5 μm. The different regions of the rat brain can be clearly differentiated in this image.

To illustrate the improved imaging with the Au_3^+ primary cluster ion source, a region of the corpus callosum was imaged (Fig. 18.11) with a 500 μm × 500 μm field of view and with 1.95 μm × 1.95 μm pixel dimensions, by raster-scanning the primary ion source. The enhanced ion yield of the Au_3^+ allows excellent imaging with similar spatial resolution to the MetA-SIMS data of Heeren et al. It should be noted that the MetA-SIMS technique has produced images for ions in the 1,000- to 1,500-Da

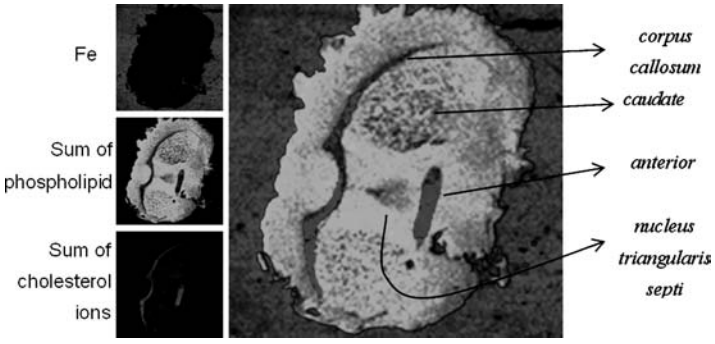

Fig. 18.10 Selected ion images obtained for stainless steel substrate, sum of characteristic phospholipid ions, sum of cholesterol ions, and a color overlay of the three images

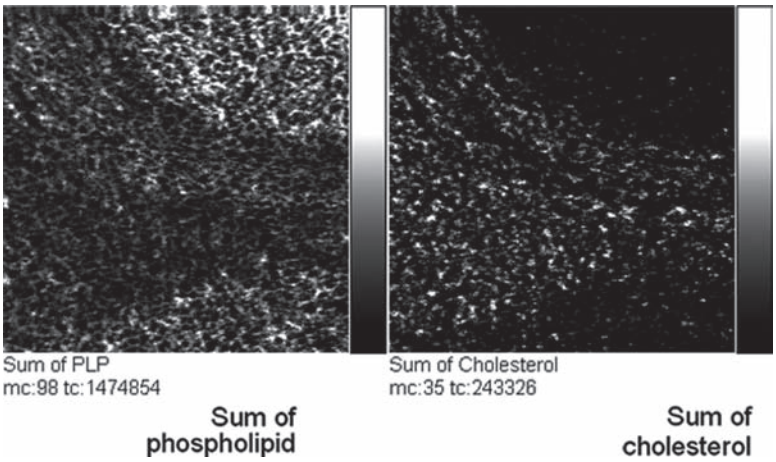

Fig. 18.11 Selected ion images obtained for the sum of characteristic phospholipid (*PLP*) ions and the sum of cholesterol ions from a region of the corpus callosum in the cross section of a rat brain. The data were acquired with an Au_3^+ primary cluster ion source raster-scanned over a 500 μm × 500 μm field of view and with 1.95 μm × 1.95 μm pixel dimensions

mass range, but the useful mass range for imaging with the Au_3^+ primary cluster ion source for tissue cross sections has been reported to be about 900 Da [22].

18.3.2 Imaging of Disease Biomarkers

The previous results demonstrate TOF-SIMS imaging spatial resolution capabilities for tissue cross sections approaching 1 μm, but the data have a limitation regarding useful mass range for imaging of <2,000 Da. These results have prompted a more narrow focus for many TOF-SIMS research groups. For many biological and medical applications based on MS, the identification of proteins and other large biomolecules is being pursued using MALDI and LC-MS/MS in conjunction with electrospray ionization techniques. The localization of metabolites and therapeutic drugs, however, represents an analytical opportunity that may more closely match the strengths of TOF-SIMS. The imaging of metabolites that are related to disease states of cells or an entire living animal has recently shown great promise; one recent application published by Laprévote et al. demonstrates the value of TOF-SIMS for MS imaging of the biomarkers of Fabry's disease [23]. Fabry's kidney disease is a lysosomal genetic disease caused by a dysfunction of α-D-galactosidase-A (α-GALA). It is linked to the X chromosome and affects 1 in 120,000 humans. The disease promotes the accumulation of glycosphingolipids Gb_3 (trihexosylceramide) and Ga_2 (digalactosylceramide) in kidney cells. The mass spectra of Gb_3 and Ga_2 are shown in Fig. 18.12, and images of Gb_3 and Ga_2 from a biopsy tissue sample of a human kidney are shown in Fig. 18.13. The imaging data were acquired

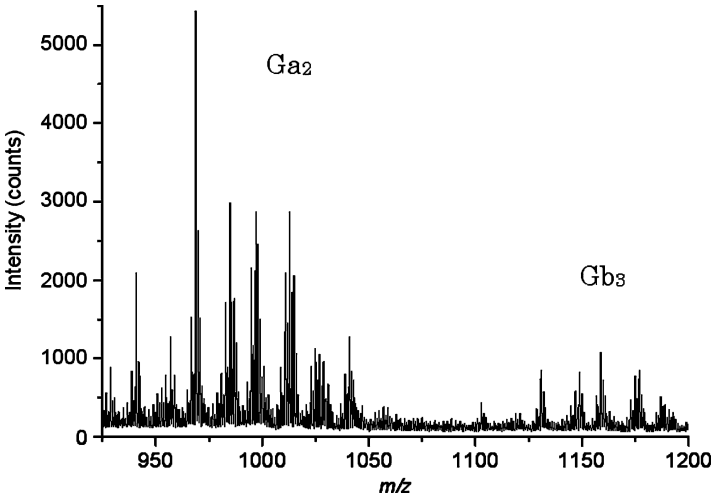

Fig. 18.12 Mass spectral data obtained with Bi_3^+ primary ion source from muscle cells for Ga_2 and Gb_3

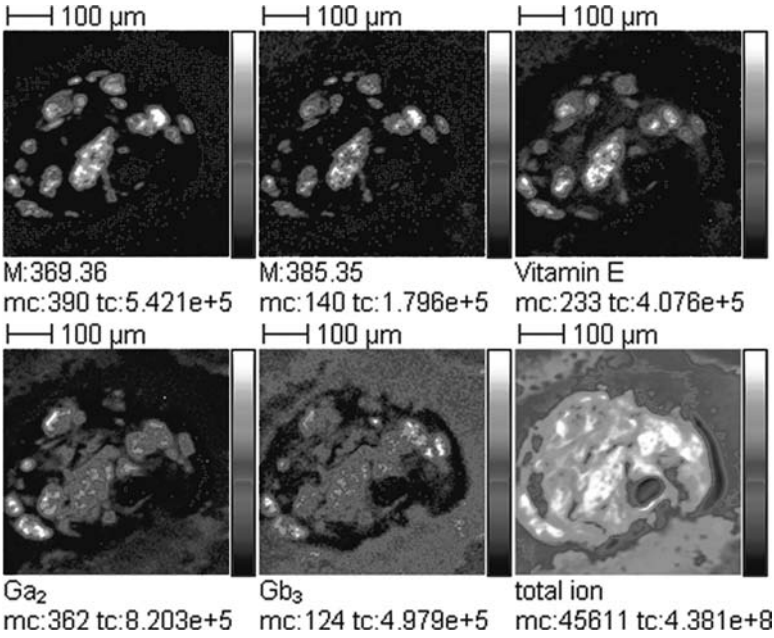

Fig. 18.13 Images of cholesterol at *m/z* 369 $(M+H-H_2O)^+$, *m/z* 385 $(M-H)^-$, vitamin E, Ga_2, and Gb_3, and total ion image obtained with Bi_3^+ primary ion source from muscle cells of Duchenne muscular dystrophy-afflicted subjects

in 30 min with a raster-scanned Bi_3^+ primary ion gun over a 500 μm × 500 μm field of view and with 1 μm × 1 μm pixel dimensions. The images in Fig. 18.13 show a colocalization of Gb_3 and Ga_2, as well as a colocalization with vitamin E, cholesterol, and cholesterol sulfate (data not shown). The authors claim an image spatial resolution for Gb_3 and Ga_2 of 1 μm. Similar imaging results of biomarkers for muscle cell samples from mice and humans suffering from Duchenne muscular dystrophy have shown the localization of cholesterol, vitamin E, and fatty acids of different chain lengths in regions of different cell types [24]. These valuable results point to the unique analytical capability of TOF-SIMS for cellular and subcellular MS imaging in supporting medical research.

18.3.3 Imaging of Drugs with Controlled Drug-Release Coatings

Presently, most therapeutic drugs have a mass <1,000 Da. Historically, most drug treatments have depended on oral ingestion or intravenous administration. The recent increase in the use of implanted medical devices has added a new dimension to the requirements for drug delivery. Despite the best efforts of material scientists to develop materials and surface coatings that are "biocompatible," the human body has a natural tendency to attack any implanted materials as foreign bodies; this is particularly evident with the increased use of stents to treat cardiovascular disease. Although the expandable stent has become a common tool in treating blockages in the heart, complications arising from the body enveloping the stent and creating new blockages in the artery causes anxiety in patients and consternation in the medical community. To prevent this process of restenosis, stent manufacturers are now developing drug-release coatings that can be applied directly to the stent. A key factor in the development of these coatings is an understanding of the 3D concentration of the drug and the pathways for drug elution from the coating. 3D MS imaging of the drug in the coating, as well as the periodic analysis of this drug composition as a function of elution of the drug, is an exciting new application of TOF-SIMS.

In a recent study by Fisher et al. [25] at Physical Electronics in Chanhassen, MN, the 3D compositional analysis of the drug Rapamycin in a soluble coating of poly(lactic-*co*-glycolic acid) deposited on a test coupon was obtained with TOF-SIMS. 2D images of the drug and coating were obtained at a series of depths from the outer surface to a depth of 3 μm into the coating, using 20-keV C_{60}^+ sputter depth profiling. The resultant collection of 2D images was combined using iso-surface 3D image display software. The results are displayed in Fig. 18.14.

To more fully understand the structure shown in Fig. 18.14, the opacity of the green iso-surface model, poly(lactic-*co*-glycolic acid), was reduced to allow the viewer to see into the coating in Fig. 18.15 [25].

This study illustrates the potential for 3D TOF-SIMS imaging of organic, biomaterial, and tissue samples, using the C_{60}^+ sputter depth profiling technique. Further studies are underway to explore the benefits of this approach with other materials, especially tissue samples.

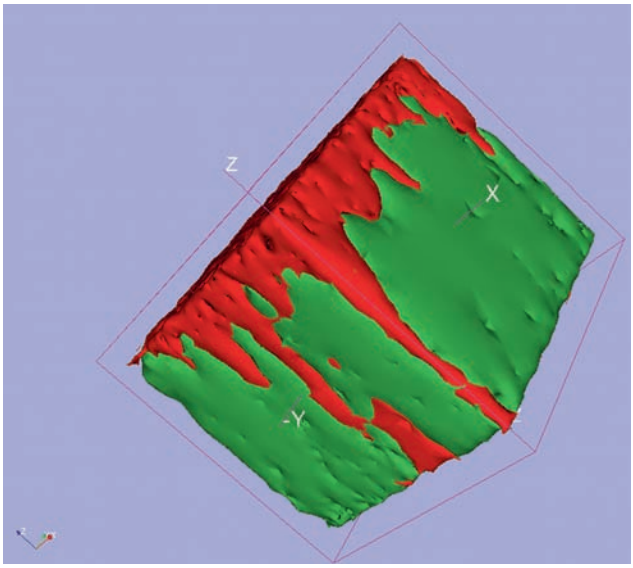

Fig. 18.14 The 3-D intensity of the drug Rapamycin (*red*) and the soluble coating poly(lactic-*co*-glycolic acid) (*green*), for a 200 μm width × 200 μm length × 2.8 μm depth

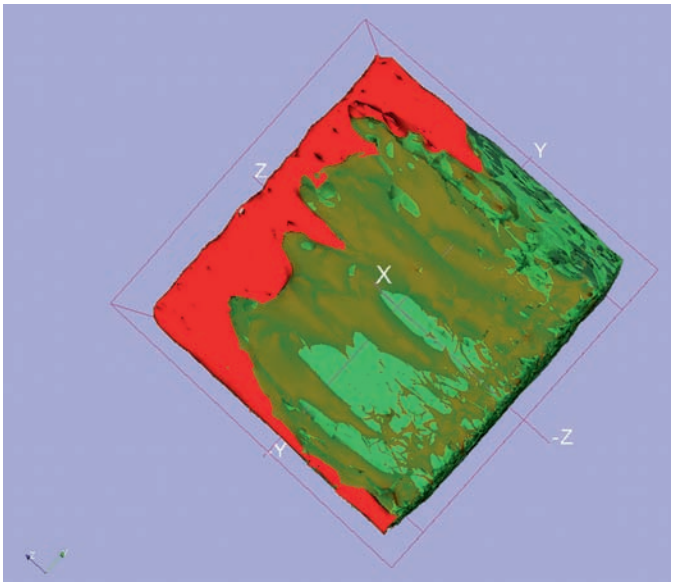

Fig. 18.15 The 3D intensity of the drug Rapamycin (*red*) and the soluble coating poly(lactic-*co*-glycolic acid) (*green*) for a 200 μm width × 200 μm × 2.8 μm depth. The opacity of the coating model (in *green*) has been reduced to allow the multiple channels in the coating to be more visible

18.4 Comparison of MALDI and TOF-SIMS

The several sections on the MALDI technique presented elsewhere in this text, together with the material discussed in this chapter regarding the TOF-SIMS technique, allow some high-level comparisons to be made between these two techniques. A summary of the characteristics by which these techniques are compared is presented in Table 18.2. From these comparisons, it should be evident that both techniques are powerful tools for MS imaging; it should also be clear that the two techniques are complementary in many ways, with the two most notable aspects being the imaging spatial resolution and the mass range of the detected ions. These two characteristics will likely allow application developments from these two techniques that are complementary. MALDI has a required position as a tool for imaging proteins and other macromolecules found in cells, and TOF-SIMS will likely develop as an imaging tool that examines disease biomarkers and the localization of therapeutic drugs. It can also be expected that further technical developments for both instruments will allow each technique to provide additional complementary and, in some cases, directly comparable data from the same samples. It can be expected that many research laboratories will use both these techniques in MS imaging.

18.5 Future Developments for TOF-SIMS

Significant technical developments will likely occur in four key areas over the next several years. The first area is new primary ion source technology; this will likely focus on different cluster ion sources, particularly for organic depth profiling. The second area is new analyzer technology. Although several universities are developing prototype analyzers, it is premature to forecast which analyzers will be introduced commercially. The third area is the incorporation of MS/MS into TOF-SIMS systems. This capability is widespread for almost all other MS systems. Finally, there is the

Table 18.2 Comparison of MALDI and TOF-SIMS capabilities

Capability	MALDI	TOF-SIMS
Incident probe	Focused laser	Focused cluster ion gun
Practical mass range (Da)	>100,000	<2,000
Spatial resolution, organics (μm)	30–50	0–5
Mass resolution (M/Δm)	~10,000	~15,000
Sampling depth (μm)	1	<1
3-D imaging	Yes, multiple sections	Yes, C_{60}^+ sputtering
Molecular spectral library	Extensive	Very limited
Usual imaging approach	Stage mapping	Scanned ion gun and stage mapping

Note: These are not theoretical limits, but widely used capabilities. Some laboratories have published findings from equipment showing enhanced capabilities with both techniques

incorporation of software to quickly and conveniently interpret and output enormous amounts of data obtained in 2D and 3D raw files. It is not unreasonable to expect that both MALDI and TOF-SIMS will continue to grow in terms of performance, commercial offerings, and laboratory use around the world.

References

1. Vickerman JC, Brown A, Reed NM (1989) Secondary ion mass spectrometry. Oxford University Press, New York
2. Vickerman JC, Briggs D, eds. (2001) ToF-SIMS: surface analysis by mass spectrometry. IM Publications, Chichester
3. Postawa Z, Czerwinski B, Szewczyk M, Smiley EJ, Winograd N, Garrison BJ (2004) J Phys Chem B 108:7832–7838
4. Delcorte A, Garrison BJ (2004) J Phys Chem B 104:6785–6800
5. Cameca nanoSIMS 50. Cameca, Gennevilliers, France
6. Physical Electronics, Chanhassen, MN, USA: unpublished results
7. ION-TOF. GmbH, Münster, Germany
8. Physical Electronics USA, Chanhassen, MN, USA and ULVAC-PHI Inc., Chigasaki, Japan
9. SurfaceSpectra, Manchester, UK
10. Gillen G, Roberson S (1998) Rapid Commun Mass Spectrom 12:1202
11. van Stipdonk MJ (2001) In: Vickerman JC, Briggs D, eds. ToF-SIMS: surface analysis by mass spectrometry. IM Publications, Chichester, pp 309–345
12. Ionoptika Ltd., Epsilon House, Chilworth Science Park, Southampton S016 7NS, UK
13. Sanada N. ULVAC-PHI Inc. Chigasaki, Japan: unpublished results
14. Fisher G. Physical Electronics Inc, Chanhassen, MN, USA: unpublished results
15. Reich DF (2001) In: Vickerman JC, Briggs D, eds. ToF-SIMS: surface analysis by mass spectrometry. IM Publications, Chichester, pp 113–135
16. Wu KJ, Odom RW (1996) Anal Chem 68:873–882
17. Altelaar AFM, Van Minnen J, Jimenez CR, Heeren RMA, Piersma SR (2005) Anal Chem 77:735–741
18. Delcorte A, Bour J, Aubriet F, Muller J-F, Bertrand P (2003) Anal Chem 75:6875–6885
19. Altelaar AFM, Klinkert I, Jalink K, de Lange RJP, Adan RAH, Heeren RMA, Piersma SR (2006) Anal Chem 78:734–742
20. Severs N, Shotton D, eds. (1995) Rapid freezing, freeze-fracture, and deep etching. Wiley-Liss, New York
21. Private communication with Kwang Jen J Wu, Lawrence Livermore National Laboratory, University of California
22. Touboul D, Halgand F, Brunelle A, Kersting R, Tallarek E, Hagenhoff B, Laprévote O (2004) Anal Chem 76:1550–1559
23. Touboul D, Roy S, Germain DP, Chaminade P, Brunelle A, Laprévote O (2007) Int J Mass Spectrom 260:158–165
24. Touboul D, Brunelle A, Halgand F, De Le Porte S, Laprévote O (2005) J Lipid Res 46:1388
25. Fisher GF. Physical Electronics Inc., Chanhassen, MN, USA